



The Quantitative Evaluation Of Primary Liver Lesions On Hepatocyte Specific Contrast Enhanced Magnetic Resonance Imaging

Primer Karaciğer Lezyonlarının Hepatosit Spesifik Kontrast Ajanlı Manyetik Rezonans Görüntülemeye Kantitatif Değerlendirmesi

Şehnaz Evrimler¹, Ayşe Say¹, Adnan Karaibrahimoğlu², Mustafa Kayan¹

¹Suleyman Demirel University, Faculty of Medicine, Department of Radiology, Isparta, Turkey.

²Suleyman Demirel University, Faculty of Medicine, Department of Biostatistics, Isparta, Turkey.

Abstract

Objective: Most of the previous researchers evaluated contrast-noise ratio, SI lesion / SI liver parenchyma, and DWI in their studies for quantitative analysis of liver lesions. We aimed to investigate the diagnostic value of the quantitative measurements with new formulas calculated on Gd-EOB-DTPA enhanced DCE-MR images with 30° and 10° FA at the hepatobiliary phase and DWI.

Material-Method: There was a total of 54 primary liver lesions; n=23 HCC in the malignant group and n=19 hemangioma, n=6 FNH, n=3 hepatic adenoma, n=3 dysplastic nodule in the benign group. Relative contrast enhancement [RCE=(HBP-Pre)/Pre], absolute contrast enhancement [ACE=(SI lesion- SI liver) / SI paravertebral muscle], absolute washout [AW=(AP-HBP)/(AP-Pre)], relative washout (RW=AP-HBP/AP) and ADC values were calculated.

Results: There was a significant difference in the quantitative measurements among the liver lesion groups. HCC demonstrated significantly higher AW and RW, lower ACE and RCE values than the benign group. The ICC values between the two FA measurements were good for RCE and RW, but not for ACE and AW. HCC demonstrated significantly lower ADC values than the benign group. According to ROC analysis, cut-off values for HCC were calculated [ACE; -3.5 (sensitivity 100%, specificity 45.6%, accuracy 68.5%), AW; 0.53 (sensitivity 87%, specificity 51.6%, accuracy 66.7%), RW; 0.105 (sensitivity 95.7%, specificity 48.4%, accuracy 68.5%), RCE; -0.03 (sensitivity 73.9%, specificity 67.7%, accuracy 70.4%), ADC; 1.09 (sensitivity 73.9%, specificity 74.2%, accuracy 74.1%)].

Conclusions: We suggest that our quantitative measurements and DWI can be useful in differentiation between HCC and other benign lesions in conflicting cases.

Keywords: Liver, Hepatocellular Carcinoma, Contrast, Quantitative.

Özet

Amaç: Literatürde araştırmacılar kontrast-gürültü oranı, SI lezyon / SI karaciğer parankimi ve DAG'yi karaciğer lezyonlarının kantitatif değerlendirilmesi için kullanmışlardır. Biz çalışmamızda Gd-EOB-DTPA kontrast ajanlı DCE-MRG'de 30° ve 10° FA ile çekilmiş hepatobiliyer faz görüntülerde yeni oluşturduğumuz formülleri kullanarak ve DAG inceleme ile yapılan kantitatif değerlendirmenin primer karaciğer lezyonları için tanısallık değerini araştırmayı amaçladık.

Materyal-Metot: 54 primer karaciğer lezyonu; malign grupta n=23 HCC, benign grupta n=19 hemangioma, n=6 FNH, n=3 hepatic adenom, n=3 displastik nodül çalışmaya dahil edildi. Relatif kontrastlanma [RCE=(HBP-Pre)/Pre], mutlak kontrastlanma [ACE=(SI lezyon- SI karaciğer) / SI paravertebral kas], mutlak yıkanma [AW=(AP-HBP)/(AP-Pre)], relatif yıkanma (RW=AP-HBP/AP) ve ADC değerleri hesaplandı.

Bulgular: Karaciğer lezyon grupları arasında kantitatif ölçümlerde anlamlı farklılık bulundu. HCC benign gruba göre daha yüksek AW and RW, düşük ACE ve RCE değerleri gösterdi. İki FA ölçümleri arasında ICC değerleri RCE ve RW ölçümleri için iyi iken, ACE ve AW değerleri için değildi. HCC benign gruba göre daha düşük ADC değerleri gösterdi. ROC analizine göre; HCC için hesaplanan kesme değerleri şu şekildedir; [ACE; -3.5 (duyarlılık %100, özgüllük %45.6, doğruluk %68,5), AW; 0,53 (duyarlılık %87, özgüllük %51,6, doğruluk %66,7), RW; 0,105 (duyarlılık %95,7, özgüllük %48,4, doğruluk %68,5), RCE; -0,03 (duyarlılık %73,9, özgüllük %67,7, doğruluk %70,4), ADC; 1,09 (duyarlılık %73,9, özgüllük %74,2, doğruluk %74,1)].

Sonuç: Kantitatif ölçüm ve DAG'nin arada kalınlan olgularda HCC ve benign karaciğer lezyon ayırımında yararlı olacağını düşünmekteyiz.

Anahtar kelimeler: Hepatoselüler Karsinom, Kantitatif, Karaciğer, Kontrast.

DOI: 10.22312/sdusbed.657795

Müracaat tarihi / Received date: 11.12.2019

Kabul tarihi / Accepted date: 04.05.2020

ORCID: ŞE 0000-0002-9907-0011, AS 0000-0002-4938-9059, AK 0000-0002-8277-0281, MK 0000-0001-5255-7132

Yazışma Adresi / Corresponding: Şehnaz Evrimler,

Suleyman Demirel University School of Medicine East Campus Çünür Street, Isparta, Turkey.

Tel: +90 246 211 20 00

Fax: +90 246 211 28 30

E-posta / E-mail: drsehnaz@gmail.com

Introduction

Magnetic Resonance Imaging (MRI) is a valuable diagnostic imaging method with high contrast resolution, the ability of morphological and functional evaluation for primary liver lesions, and lack of ionizing radiation exposure (1, 2). Diffusion-Weighted Imaging (DWI) and dynamic contrast-enhanced imaging (DCE) enable to make both qualitative and quantitative evaluation (3). Hepatocyte specific contrast-enhanced MRI is beneficial in the characterization of atypical focal liver lesions (4). Gd-EOB-DTPA (gadoteric acid disodium) demonstrates similar characteristics with other extracellular contrast agents in vascular phases but shows hepatocellular uptake and biliary excretion at the hepatobiliary phase (HBP) (5, 6). The quantitative evaluations have been commonly used in dynamic contrast-enhanced breast MR and oncological MR imaging by the calculation of the plot of signal intensity (SI) versus time, the initial area (integral) under the time signal curve (AUC). Time to peak, maximum SI, washout ratios are calculated by semiquantitative methods (7, 8). Contrast-noise ratio ($CNR = \frac{SI_{\text{tumour}} - SI_{\text{liver}}}{SI_{\text{background noise}}}$), enhancement ratio ($ER = \frac{SI_{\text{postcontrast}}}{SI_{\text{precontrast}} \times 100}$), or contrast enhancement ratio ($CER = \frac{SI_{\text{liver}} - SI_{\text{lesion}}}{SI_{\text{paravertebral muscle}}}$) were calculated for quantitative analysis of liver lesions in the previous studies (9-12). Okada et al. declared that FA ranging from 10° to 20° at the hepatobiliary phase is successful in diagnosis of HCC and metastasis (13). It was stated that the diagnostic performance of images with flip angle (FA) 30° were better than images with FA 10° and earlier images with FA 30° demonstrated equal or better performance compared with later images with FA 10° (9, 14, 15).

Cirrhosis associated benign nodules are <2 cm, iso-hyperintense on T1WI, iso-hypointense on T2WI, and isointense on DWI. Steatotic nodules show a signal loss on out-of-phase images compared with in-phase images. Iron-containing or siderotic nodules exhibit hypointensity on T2WI/T2*WI (16). Benign nodules demonstrate isointense contrast-enhancement with the parenchyma at the arterial and venous phase. Some of them can show hyperenhancement on the arterial phase and become isointense with a washout at the venous phase but show isointense enhancement at HBP (16-19).

Hepatocellular carcinoma (HCC) generally demonstrate hypointensity on T1WI but also may show hyperintensity. They are hyperintense on T2WI, but the well-differentiated ones may be iso-hyperintense. HCC lesions can also show steatotic or hemorrhagic characteristics (16). They are hyperattenuated at the arterial phase and show washout in 80%. Less than 20% of HCCs are well-differentiated and do not show hyperenhancement (20). Tumor capsule and nodule in nodule appearance are other features that may be observed in HCCs. The capsule enhances more than the parenchyma at the late phase. They are hypointense at HBP. The amount of hypointensity depends on the concentration and function of Organic Anion Transporting Polypeptide (OATP) and Multidrug Resistance Associated Protein (MRP). Hyperintense lesions are usually benign (21, 22).

Hemangiomas demonstrate hypointensity on T1WI and hyperintensity on T2WI (16). They show typical peripheral nodular centripetal progressive contrast enhancement. The contrast enhancement follows the blood pool. Smaller lesions may demonstrate flash filling enhancement. Some lesions may show late enhancement. Larger lesions may show non-uniform contrast enhancement. A central scar may be observed in some lesions (16). They demonstrate pseudo washout and become hypointense at HBP. Malign lesions show washout earlier than the vessel (23).

Focal nodular hyperplasia (FNH) is hypo-isointense on T1WI, mildly hyperintense-isointense on T2WI. The central scar is hyperintense on T2WI (16). They show hyperenhancement at the arterial phase, become isointense at later phases, while central scar shows progressive enhancement and becomes iso-hyperintense at HBP (24, 25).

Hepatic adenomas are generally well-defined and hyper-isointense lesions on T1WI, mildly hyperintense on T2WI. They can show hemorrhagic changes. Fat may be seen in hepatic adenomas. Calcification is rarely seen in these lesions (16). They demonstrate moderate arterial enhancement at the arterial phase, show washout at the portal phase, and become isointense. They are seen as hypointense lesions at HBP, but some can show mild or peripheral enhancement (16).

The purpose of our study was to evaluate the diagnostic value of absolute washout (AW), relative washout (RW), absolute contrast enhancement (ACE), and relative contrast enhancement (RCE) in the quantitative evaluation of primary liver lesions on Gd-EOB-DTPA enhanced MR images with FA 30° and FA 10° .

Material and Methods

Patient Population and Ethics

Gd-EOB-DTPA enhanced abdomen MR images of 54 patients with primary liver lesions obtained between 2013-2018 were included in our retrospective, waiving informed consent, and institutional review board-approved study. 53.7% of patients were male (n=29), 46.3% were female (n=25). The size of the lesions ranged between 5mm-30mm. 42.6% of the lesions were HCC (n=23) in the malignant group. Benign group (57.4%, n=31) was composed of hemangioma (n=19), FNH (n=6), hepatic adenoma (n=3), and dysplastic nodule (n=3).

Image Acquisition and Analysis

Images were obtained by 1.5T MR magnet (Magnetom Avanto, Siemens Healthcare Sector, Erlangen, Germany). Imaging parameters were as follows; 1) DWI: single-shot echo planar diffusion weighted imaging with b values of 0, 50 and 800 s/mm² TR/TE 8260.4/75 ms, acquisition time 1926150, FoV 3796308, parallel imaging acceleration factor 2) during free-breathing, pre and post-contrast T1-weighted images were obtained. 0.025mmol/kg Gd-EOB-DTPA (gadoteric acid disodium) was administered. Post-contrast images were obtained at 25 seconds (arterial phase), 60 seconds (portal venous phase), and 80 seconds (late venous phase). HBP imaging was obtained at 20min with FA 30° and FA 10° .

Images were evaluated with Picture Archiving and

Communication System (PACS), OsiriX MD v. 10.0.2 software, (UCLA, Pixmeo), GPL licensed free access resource code and commercially licensed, FDA approved Mac OS X radiology workstation. The maximum region of interest (ROI) was drawn on lesions as large as possible for signal intensity and ADC measurements. Measurements from cystic-necrotic areas and vascular structures were avoided.

In cirrhotic liver parenchyma, the parenchymal liver intensity measurements were performed from the region without regenerative nodule as much as possible.

The quantitative measurement formulas were as follows; Relative Contrast-Enhancement (RCE)=HBP-Pre/Pre, Absolute Contrast-Enhancement at HBP (ACE)=SI lesion-SI liver / SI paravertebral muscle, Absolute Washout (AW)=AP-HBP/AP-Pre, Relative Washout (RW)=AP-HBP/AP (SI: signal intensity, AP: arterial phase, Pre: pre-contrast). Dynamic contrast enhancement (SI-time) curves were drawn and classified as type-1; persistent enhancement, type-2; firstly increasing enhancement, then showing plateau, type-3; rapid enhancement in the beginning, then showing washout with time. Diffusion-weighted images (DWI) were scored by subjective evaluation for diffusion restriction as definite:2, suspected:1, none:0. In addition, ADC values were calculated by ROI replacement.

Statistical Analysis

Statistical analyses of the study were performed by SPSS (IBM Inc., Chicago, IL, USA) with version 20.0. Power analysis was performed by GPower software (Ver 3.1.9.2, Kiel, Germany). The number of patients required for the study was determined by power analysis for Chi-square analysis with 5% error, and 80% power. Groups were determined

by the single blinding method. Descriptive statistics were presented as frequencies (percentage) for categorical variables; as mean±SD for numerical variables. Continuous variables were analyzed for normality by the Kolmogorov-Smirnov and Shapiro-Wilk test. Since the distributions of the measurements were not normal, the Mann-Whitney U test for two independent samples and the Kruskal-Wallis test for multiple samples were used for group comparison. Kruskal-Wallis post-hoc test was applied for significant results. The associations between variables amongst categorical data were determined by corrected Chi-square analysis. ICC (Intraclass Correlation Coefficient) was calculated for the evaluation of intraobserver reliability. Logistic regression analysis was done for the detection of the effect of variables on the diagnosis. A p-value of less than 0.05 (p<0.05) was considered statistically significant by taking 5% for type-I error.

Results

ACE, RCE, AW, and RW were significantly different in all of the primary liver lesion groups on images with FA30° (Table 1). All of the quantitative measurements except ACE on images with FA10° were significantly different among the primary liver lesion groups (Table 2).

According to the quantitative measurements on images with FA30°, ACE was highest in hemangioma and lowest in FNH. RCE was lowest in HCC and highest in FNH. AW was highest in HCC, RW was highest in hepatic adenoma (Table 1).

According to the quantitative measurements on images with FA10°, ACE was highest in hemangioma, lowest in HCC. RCE was lowest in the dysplastic nodule, highest in FNH. AW and RW were highest in hepatic adenoma (Table 2).

Table 1. The quantitative measurements on images with FA30°

FA 30°	Hepatic adenoma (n=3)	DN ^a (n=3)	FNH ^b (n=6)	HCC ^c (n=23)	Hemangioma (n=19)	p
	(Mean±Sd)	(Mean±Sd)	(Mean±Sd)	(Mean±Sd)	(Mean±Sd)	
ACE ¹	-2.50±3.54	-1.28±0.81	-0.77±0.92	-1.59±0.99	-3.62±2.08	<0.001*
RCE ²	0.07±0.43	-0.05±0.26	0.68±0.28	-0.08±0.33	0.12±0.54	0.013*
AW ³	0.52±1.03	1.47±1.06	-1.11±2.50	1.36±1.22	0.73±3.52	0.030*
RW ⁴	0.38±0.48	0.20±0.21	-0.04±0.24	0.37±0.16	0.11±0.45	0.010*

¹Absolute contrast enhancement, ²Relative contrast enhancement, ³Absolute washout, ⁴Relative washout

^aDysplastic nodule, ^bFocal nodular hyperplasia, ^cHepatocellular carcinoma

*statistically significant

Table 2. The quantitative measurements on images with FA10°

FA 10°	Hepatic adenoma (n=3)	DN ^a (n=3)	FNH ^b (n=6)	HCC ^c (n=23)	Hemangioma (n=19)	p
	(Mean±Sd)	(Mean±Sd)	(Mean±Sd)	(Mean±Sd)	(Mean±Sd)	
ACE ¹	-0.63±0.55	-0.58±0.33	-0.54±0.31	-0.46±0.46	-0.95±0.51	0.062
RCE ²	0.60±0.26	0.30±0.22	0.83±0.22	0.44±0.34	0.79±0.27	<0.001*
AW ³	0.01±1.12	-0.75±0.38	-1.88±3.00	-0.01±0.83	-4.32±4.20	<0.001*
RW ⁴	0.15±0.40a	-0.09±0.05	-0.14±0.28	0.01±0.17	-0.42±0.35	0.001*

¹Absolute contrast enhancement, ²Relative contrast enhancement, ³Absolute washout, ⁴Relative washout

^aDysplastic nodule, ^bFocal nodular hyperplasia, ^cHepatocellular carcinoma

*statistically significant

Table 3. The quantitative measurements of benign liver lesion group and malignant liver lesion group (HCC) on images with FA 30°

	Benign (n=31)	Malignant (n=23)	p
	(Mean±Sd)	(Mean±Sd)	
ACE ¹ FA ⁵ 30	-2.73±2.26	-1.59±0.99	0.032*
RCE ² FA ⁵ 30	0.21±0.51	-0.08±0.33	0.020*
AW ³ FA ⁵ 30	0.42±3.05	1.36±1.22	0.034*
RW ⁴ FA ⁵ 30	0.11±0.40	0.37±0.16	0.020*
ACE ¹ FA ⁵ 10	-0.80±0.48	-0.46±0.46	0.019*
RCE ² FA ⁵ 10	0.73±0.29	0.44±0.34	<0.001*
AW ³ FA ⁵ 10	-3.08±3.86	-0.01±0.83	0.001*
RW ⁴ FA ⁵ 10	-0.28±0.37	0.001±0.17	0.003*

¹Absolute contrast enhancement, ²Relative contrast enhancement, ³Absolute washout, ⁴Relative washout, ⁵Flip angle
*statistically significant

Table 4. The intercorrelation coefficient (ICC) values between the two flip angle measurements

FA 30°-FA 10°	ICC
Absolute Contrast Enhancement	0.465
Relative Contrast Enhancement	0.779
Absolute Washout	0.376
Relative Washout	0.791

HCC (malignant group) demonstrated significantly higher AW and RW, lower ACE and RCE values than benign lesion group (Table 3).

The intercorrelation coefficient (ICC) values between the two flip angle measurements were good for RCE and RW, but not for ACE and AW (Table 4).

Type 3 enhancement pattern was the most observed enhancement pattern (n=39, 72%). Type 2 enhancement was observed in 8 (14%) patients and type 1 enhancement was observed in 7 patients (14%). The quantitative measurements were evaluated according to enhancement patterns. According to measurements on images with FA 30°, RCE was higher in type-1 and-2, and negative in type-3 enhancement group. AW and RW were significantly higher in type 3 group. According to the measurements on images with FA 10°, ACE was highest in type-3, but it was not statistically significant. RCE was highest, but AW and RW were significantly lower in type-1 enhancement group.

Table 5. ADC values according to benign and malignant groups and liver lesion groups

ADC ¹	Benign (n=31)	Malignant (n=23)					p
	(Mean±Sd)	(Mean±Sd)					
	1.44±0.48	1.04±0.49					0.002*
	Hepatic adenoma (n=3)	DN ^a (n=3)	FNH ^b (n=6)	HCC ^c (n=23)	Hemangioma (n=19)		
	(Mean±Sd)	(Mean±Sd)	(Mean±Sd)	(Mean±Sd)	(Mean±Sd)	p	
ADC ¹	1.48±0.53	0.85±0.05	0.96±0.20	1.04±0.49	1.68±0.38	<0.001*	

¹Apparent Diffusion Coefficient,

^aDysplastic nodule, ^bFocal nodular hyperplasia, ^cHepatocellular carcinoma

*statistically significant

There was no significant difference in ADC values between contrast enhancement types (p=0.138). ADC was highest in hemangioma and lowest in the dysplastic nodule. There was a significant difference in ADC between hemangioma and dysplastic nodule and FNH (p<0.001). There was no significant difference in visual DWI assessment between the groups (p=0.791). We observed a significant difference when we compared the benign group with the malignant group (p=0.002). HCC group demonstrated significantly lower ADC values than the benign group (Table 5).

We calculated cut-off values of quantitative measurements of HCC and benign lesion groups on images with FA30° according to ROC analysis (Table 6).

The effect of the quantitative measurements on malignancy diagnosis was evaluated by logistic regression. RW, ACE, ADC and type-2 enhancement demonstrated significant logistic regression analysis. RW and ACE showed positive, whereas ADC and type-2 enhancement pattern showed a negative odds ratio on the malignancy (Table 7).

Table 6. The cut-off values of quantitative measurements for differentiation between malignant and benign liver lesion groups on images with FA 30° according to ROC analysis

Variables	Cut-off	Sensitivity	Specificity	Accuracy
ACE ¹	-3.5	100%	45.60%	68.52%
AW ²	0.525	86.96%	51.61%	66.67%
RW ³	0.105	95.65%	48.39%	68.52%
RCE ⁴	-0.03	73.91%	67.74%	70.37%
ADC ⁵	1.085	73.91%	74.19%	74.07%

¹Absolute contrast enhancement, ²Absolute washout, ³Relative washout, ⁴Relative contrast enhancement, ⁵Apparent diffusion coefficient

Table 7. Logistic regression analysis for HCC

Malignancy	p	OR	95%CI
RW ¹ FA ⁴ 30°	0.045	15250.8	1.239-42723.6
ACE ² FA ⁴ 30°	0.012	4.512	1.395-14.597
ADC ³	0.018	-333.3	3.04-534.6
Type-2 contrast-enhancement	0.036	-998.5	2.17-1245.6

¹Relative washout, ²Absolute contrast enhancement, ³Apparent diffusion coefficient, ⁴Flip angle

Discussion

MR imaging gives us both morphologic and functional information in the assessment of primary liver lesions. DWI and multiphasic dynamic contrast-enhanced imaging enable us to make both qualitative and quantitative assessments (1-3). Hepatocyte specific contrast-enhanced MR is useful for atypical cases with a diagnostic dilemma (4). Gd-EOB-DTPA shows similar characteristics with other extracellular contrast agents in vascular phases, but also shows hepatocellular uptake and biliary excretion later in the HBP (5, 6). OATPs are actively transported from sinusoidal space to hepatocytes via the lipophilic EOB group. Liver parenchyma starts to enhance strongly 1-2 min after the intravenous administration of the contrast agent. It reaches the maximum enhancement approximately at 20 min and continues for 2 hours. The contrast agent is excreted to biliary canals by MRPs and observed earliest, 5-10 min after contrast agent administration (26, 27). It is eliminated by the biliary system in 43.1–53.2% and the renal excretory system in 41.6–51.2% (28, 29). DCE-MRI provides quantitative values for tumor vascularity and angiogenesis. These values can be used for treatment response assessment and prognosis prediction, especially for HCC (30).

We classified primary liver lesions based on signal intensities on T1WI, T2WI and post-contrast images [Figure 1 (A-D), 2 (A-D), 4 (A-D), 5(A-D)]. In addition, we calculated RCE, ACE, AW, and RW at HBP. Dynamic contrast enhancement curves were drawn [Figure 1 (E), 2 (E), 4 (E), 5 (E)]. DWI was evaluated both visually and quantitatively by measuring the ADC values [Figure 3 (A-D)].

Contrast-Noise Ratio [$CNR=(SI_{liver}-SI_{lesion}) / SI_{noise}$] at HBP was measured in previous studies. CNR calculated on 5min-FA30°, 10min-FA30° images were similar or higher in comparison with 20min-FA10° (9, 14, 15). Therefore, we firstly obtained 20min-FA30°, then FA10° with approximately 1min delay.

Frericks et al. calculated liver parenchyma signal-noise ratios (SNRs), liver/lesion contrast-noise ratios (CNRs), and enhancement ratio [$ER=(SI_{post-contrast}-SI_{pre-contrast}) / SI_{pre-contrast} \times 100$] of 25 HCC lesions. HCC demonstrated positive CNR at the arterial phase and negative but absolute higher CNR at the progressive phases. The maximum absolute CNR was found at 20 min. They didn't find a correlation between contrast-enhancement degree and tumor grade. Liver / lesion contrast ratio was highest on images at 20 min (10). Kim et al. calculated contrast-enhancement ratios [$CER=(SI_{liver}-SI_{lesion}) / SI_{paravertebral\ muscle}$] (11). In our study, we calculated ACE at HBP similar to CNR in Frericks et al.'s and CER in Kim et al.'s study. We found negative values for ACE of HCC. HCC demonstrated lower absolute values than the benign group. There was a significant difference among the liver lesion groups in ACE calculations on images with FA30°, while there was not on images with FA10°. ACE was highest in hemangiomas on images with both angles. The intercorrelation coefficient values of ACE and AW between the two FA were low.

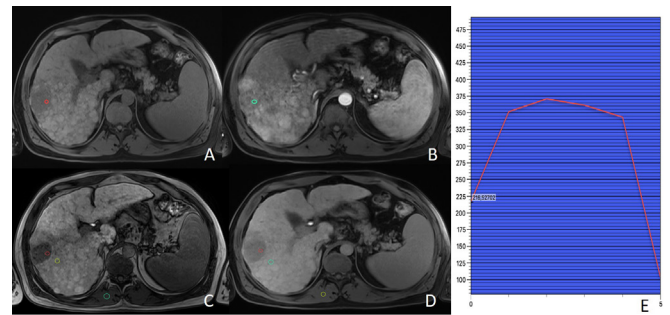


Figure 1. A HCC lesion was seen in segment 6 of a cirrhotic liver with hypointensity on axial FS T1WI (A), hyperenhancement at arterial phase (B), showing washout at hepatobiliary phase on the image with FA30°(C), and FA10° (D). The dynamic contrast-enhancement curve (E) was type-3

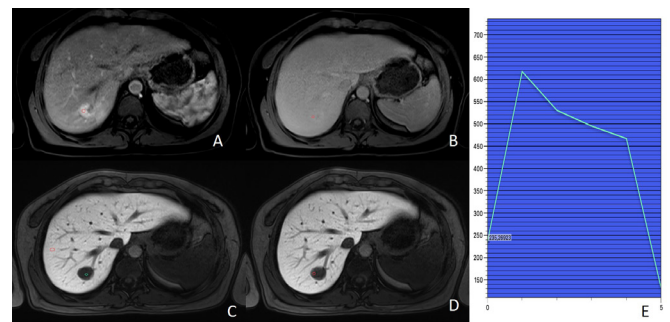


Figure 2. A hepatic adenoma was seen in segment 7 as a hyperintense lesion on axial FS T1WI at arterial phase(A), showing washout at portal phase and became isointense(B), then hypointense at hepatobiliary phase on the image with FA30°(C), and FA10° (D). The dynamic contrast-enhancement curve (E) was type-3

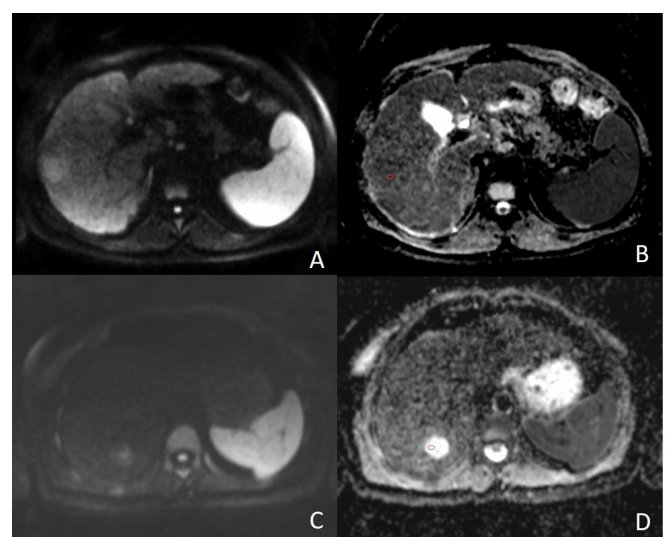


Figure 3. DWI b 800 (A) ve ADC (B) images of the HCC lesion in Figure 1. The lesion showed diffusion restriction in visual assessment and ADC was calculated as 0.89 mm²/sn DWI b 800 (C) ve ADC (D) images of hepatic adenoma lesion in Figure 2 didn't show diffusion restriction in visual assessment and ADC was calculated as 2.2 mm²/sn

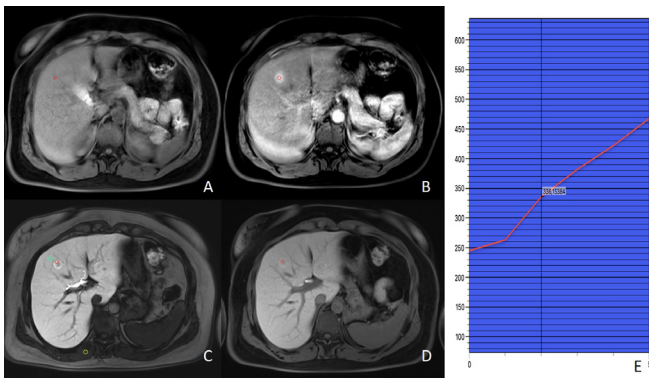


Figure 4. A FNH was seen as an isointense lesion on axial FS T1WI (A), and became hyperattenuated at arterial phase (B), then kept showing hyperenhancement on images with FA30°(C) and FA 10° (D) at hepatobiliary phase. The dynamic contrast-enhancement curve (E) was type-1

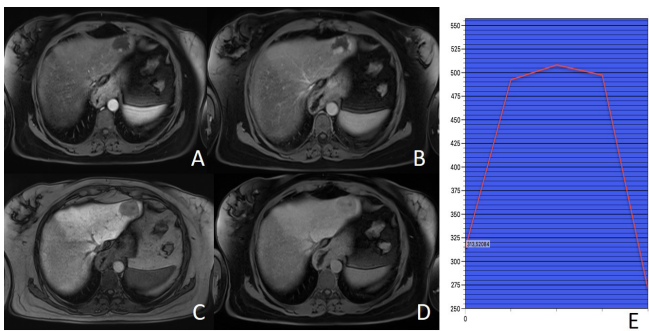


Figure 5. A hemangioma in segment 2 with peripheral nodular centripetal progressive enhancement on axial FS T1WI at arterial phase (A), portal phase (B) showed washout on images with FA 30°(C) ve FA 10° (D) at hepatobiliary phase and became hypointense. The dynamic contrast-enhancement curve (E) was type-3

Morelli et al. calculated enhancement ratio [ER=(SI lesion postcontrast-SI precontrast) / SI precontrast], and contrast ratio (CR=SI lesionx / SI liverx, x for pre-post contrast phase). They concluded that HBP MRI was superior to ADC and contrast enhancement per time values of conventional dynamic contrast-enhanced MR. They observed ER was superior to CR in the diagnosis of HCC, but CR was superior in differentiation between hepatic adenoma and FNH (12). We calculated RCE, a similar calculation to the ER that Morelli et al. studied at the HBP. RCE was lowest in HCC and highest in FNH on images with both FA. There was a significant difference in RCE among liver lesion groups. HCC group had significantly lower RCE than the benign lesion group. The intercorrelation coefficient values of RCE between the two FA was high.

Hyperenhancement at arterial phase and washout were accepted as specific criteria for HCC, but the quantitative evaluation of washout is rare in the literature. Kloeckner et al. conducted a study on patients with liver transplantation or HCC resection to find a cut-off value for the objective diagnosis of HCC. They calculated the percentage signal ratio [PSR=100x (Adjacent SI / Liver SI)] without using a hepatocyte-specific contrast agent. They declared that PSR was an easy and reproducible formula to calculate the

washout quantitatively for HCC diagnosis objectively (31). We calculated AW and RW ratios to find the washout ratio of the contrast enhancement objectively. These formulas have not been used for liver lesions before, as far as we know. There was a significant difference in AW and RW ratios between the liver lesion groups. AW was highest in HCC and RW was highest in hepatic adenoma on images with FA30°. Both AW and RW were found highest in hepatic adenoma on images with FA10°. Malignant (HCC) group showed significantly higher AW and RW ratios than the benign group on images with both flip angles. The ICC values between the two FA angle quantitative measurements were good for RW, but not for AW.

There was no significant difference in dynamic contrast enhancement curves between liver lesion groups. However, hepatic adenoma, hemangioma, dysplastic nodule, and HCC demonstrated mostly type 3 enhancement pattern. FNH showed type-1 and type-2 enhancement patterns. To the best of our knowledge, there has been no previous study investigating the contrast enhancement curve types in liver lesion diagnosis. The quantitative measurement analysis according to the enhancement curve types showed that RCE was higher in type-1, type-2 and had negative mean value in type-3 on images with FA30°. AW and RW were significantly high in the type-3 group. ACE was highest in type 3 group on images with FA10°, but it was not statistically significant. RCE was high in type-1, AW and RW were significantly low in the type-1 group on images with FA10.

DWI with high b values ($\geq 500\text{s/mm}^2$) can be used to differentiate between solid and cystic lesion by visual assessment. The quantitative ADC values are used for differential diagnosis between benign and malign lesions. The benign lesions have higher, malign lesions have lower ADC values, but overlapping in values can be observed. For example; mucinous or necrotic malignant tumors can demonstrate high ADC values. Solid benign lesions and abscess can have low ADC values. Various ADC cut-off values ($1.4\text{--}1.6 \times 10^{-3} \text{mm}^2/\text{s}$) with sensitivity ranging between 74-100% have been defined in the literature (1). Previous studies declared ADC cut-off values as $0.94\text{--}2.85 \times 10^{-3} \text{mm}^2/\text{s}$ for metastasis and $0.69\text{--}2.28 \times 10^{-3} \text{mm}^2/\text{s}$ for liver parenchyma. The variability in ADC values depends on different b-values, breath-hold, respiratory-triggered, navigator-echo techniques. Although DWI alone is not adequate to characterize the lesion, it increases the diagnostic accuracy when combined with dynamic contrast-enhanced MRI (32-34). DWI has a high negative predictive value for HCC and avoids unnecessary invasive procedures (33). We observed that the lesions with absolute or suspected diffusion restriction visually had lower ADC values than the lesions without diffusion restriction visually. There was no significant difference in DWI evaluation between the lesion groups and groups according to the dynamic contrast-enhancement curve types. However, the malignant group showed diffusion restriction and had lower ADC values than the benign group significantly. ADC was highest in hemangioma and lowest in the dysplastic nodule. The mean value of ADC for HCC was $1.04 \pm 0.49 \text{mm}^2/\text{sec}$. It

was mentioned that both visual and quantitative assessment of DWI were useful for differentiation of hemangioma and cyst from malignant lesions, but some benign lesions like FNH and hepatic adenoma can show overlapping in ADC values with the malignant lesions. Morelli et al. declared that hemangioma had higher ADC values than the other lesions (12). We also observed that hemangiomas had a higher mean ADC value ($1.68 \pm 0.38 \text{ mm}^2/\text{sec}$) than the other primary liver lesions.

The cut-off values of quantitative measurements for differentiation between malignant and benign liver lesion groups on images with FA 30° were calculated according to ROC analysis. We observed high sensitivity ratios for ACE, AW, and RW. These quantitative measurements showed higher diagnostic performance than RCE and ADC.

The factors associated with malignancy were evaluated by ordinal logistic regression analysis and the goodness of fit was statistically significant. RW and ACE had positive, ADC and type-2 contrast-enhancement had a negative association with HCC.

The limitations of the study were as follows; 1) retrospective analysis, 2) only primary liver lesions were included; we excluded the metastatic lesions because they can have different contrast-enhancement and signal intensity depending on the origin of the primary tumor, 3) most of the lesions did not have histopathological confirmation, because these patients had follow-up imaging and radiological-clinical-laboratory findings were enough for diagnosis without a need for invasive procedure. Only 6 of them had a histopathological diagnosis and all of them were HCC.

Conclusion

It was stated that the diagnostic performance of images with FA 30° was better than the images with FA 10° in the literature. They measured contrast-noise ratio and SI lesion / SI liver at HBP in most of the previous studies. We observed significant differences in ACE, RCE, AW, and RW calculations on images with both flip angles between HCC and the benign liver lesion group. The cut-off values of these measurements showed high sensitivity ratios. Both visual and quantitative assessment of DWI showed a significant difference in HCC diagnosis. Therefore, we suggest that the quantitative assessment can help in differentiating HCC from the other benign liver lesions in conflicting cases, but further studies with a larger patient population are recommended.

The abstract of the study was orally presented in the congress of Turkish Society of Magnetic Resonance (TMRD 2019) (SS 011-Oral presentation).

References

- Chandarana H, Taouli B. Diffusion and perfusion imaging of the liver. *European journal of radiology*. 2010;76(3):348-58.
- Low RN. Abdominal MRI advances in the detection of liver tumours and characterisation. *The Lancet Oncology*.

2007;8(6):525-35.

- Pirasteh A, Clark HR, Sorra EA, Pedrosa I, Yokoo T. Effect of steatosis on liver signal and enhancement on multiphasic contrast-enhanced magnetic resonance imaging. *Abdominal Radiology*. 2016;41(9):1744-50.
- Jeong WK, Kim YK, Song KD, Choi D, Lim HK. The MR imaging diagnosis of liver diseases using gadoteric acid: emphasis on hepatobiliary phase. *Clinical and molecular hepatology*. 2013;19(4):360.
- Lee NK, Kim S, Lee JW, Lee SH, Kang DH, Kim GH, et al. Biliary MR imaging with Gd-EOB-DTPA and its clinical applications. *Radiographics*. 2009;29(6):1707-24.
- Reimer P, Schneider G, Schima W. Hepatobiliary contrast agents for contrast-enhanced MRI of the liver: properties, clinical development and applications. *European radiology*. 2004;14(4):559-78.
- Evelhoch JL. Key factors in the acquisition of contrast kinetic data for oncology. *Journal of Magnetic Resonance Imaging: An Official Journal of the International Society for Magnetic Resonance in Medicine*. 1999;10(3):254-9.
- Kuhl CK, Mielcareck P, Klaschik S, Leutner C, Wardelmann E, Gieseke J, et al. Dynamic breast MR imaging: are signal intensity time course data useful for differential diagnosis of enhancing lesions? *Radiology*. 1999;211(1):101-10.
- Cho E-S, Yu J-S, Park AY, Woo S, Kim JH, Chung J-J. Feasibility of 5-minute delayed transition phase imaging with 30° flip angle in gadoteric acid-enhanced 3D gradient-echo MRI of liver, compared with 20-minute delayed hepatocyte phase MRI with standard 10° flip angle. *American Journal of Roentgenology*. 2015;204(1):69-75.
- Frericks BB, Loddenkemper C, Huppertz A, Valdeig S, Stroux A, Seja M, et al. Qualitative and quantitative evaluation of hepatocellular carcinoma and cirrhotic liver enhancement using Gd-EOB-DTPA. *American Journal of Roentgenology*. 2009;193(4):1053-60.
- Kim MY, Kim YK, Park HJ, Park MJ, Lee WJ, Choi D. Diagnosis of focal liver lesions with gadoteric acid-enhanced MRI: Is a shortened delay time possible by adding diffusion-weighted imaging? *Journal of Magnetic Resonance Imaging*. 2014;39(1):31-41.
- Morelli JN, Michaely HJ, Meyer MM, Rustemeyer T, Schoenberg SO, Attenberger UI. Comparison of dynamic and liver-specific gadoteric acid contrast-enhanced MRI versus apparent diffusion coefficients. *PloS one*. 2013;8(6):e61898.
- Okada M, Wakayama T, Yada N, Hyodo T, Numata K, Kagawa Y, et al. Optimal flip angle of Gd-EOB-DTPA-enhanced MRI in patients with hepatocellular carcinoma and liver metastasis. *Abdominal imaging*. 2014;39(4):694-701.
- Jeon I, Cho E-S, Kim JH, Kim DJ, Yu J-S, Chung J-J. Feasibility of 10-Minute Delayed Hepatocyte Phase Imaging Using a 30° Flip Angle in Gd-EOB-DTPA-Enhanced Liver MRI for the Detection of Hepatocellular Carcinoma in Patients with Chronic Hepatitis or Cirrhosis. *PloS one*. 2016;11(12):e0167701.

15. Lee D, Cho E-S, Kim DJ, Kim JH, Yu J-S, Chung J-J. Validation of 10-Minute Delayed Hepatocyte Phase Imaging with 30 Flip Angle in Gadoteric Acid-Enhanced MRI for the Detection of Liver Metastasis. *PloS one*. 2015;10(10):e0139863.
16. Campos JT, Sirlin CB, Choi J-Y. Focal hepatic lesions in Gd-EOB-DTPA enhanced MRI: the atlas. *Insights into imaging*. 2012;3(5):451-74.
17. Cruite I, Schroeder M, Merkle EM, Sirlin CB. Gadoteric acid-enhanced MRI of the liver: part 2, protocol optimization and lesion appearance in the cirrhotic liver. *American Journal of Roentgenology*. 2010;195(1):29-41.
18. Roncalli M, Roz E, Coggi G, Di Rocco MG, Bossi P, Minola E, et al. The vascular profile of regenerative and dysplastic nodules of the cirrhotic liver: implications for diagnosis and classification. *Hepatology*. 1999;30(5):1174-8.
19. Tajima T, Honda H, Taguchi K, Asayama Y, Kuroiwa T, Yoshimitsu K, et al. Sequential hemodynamic change in hepatocellular carcinoma and dysplastic nodules: CT angiography and pathologic correlation. *American Journal of Roentgenology*. 2002;178(4):885-97.
20. Hanna RF, Aguirre DA, Kased N, Emery SC, Peterson MR, Sirlin CB. Cirrhosis-associated hepatocellular nodules: correlation of histopathologic and MR imaging features. *Radiographics*. 2008;28(3):747-69.
21. Huppertz A, Haraida S, Kraus A, Zech CJ, Scheidler J, Breuer J, et al. Enhancement of focal liver lesions at gadoteric acid-enhanced MR imaging: correlation with histopathologic findings and spiral CT—initial observations. *Radiology*. 2005;234(2):468-78.
22. Shimofusa R, Ueda T, Kishimoto T, Nakajima M, Yoshikawa M, Kondo F, et al. Magnetic resonance imaging of hepatocellular carcinoma: a pictorial review of novel insights into pathophysiological features revealed by magnetic resonance imaging. *Journal of hepato-biliary-pancreatic sciences*. 2010;17(5):583-9.
23. Doo KW, Lee CH, Choi JW, Lee J, Kim KA, Park CM. “Pseudo washout” sign in high-flow hepatic hemangioma on gadoteric acid contrast-enhanced MRI mimicking hypervascular tumor. *American Journal of Roentgenology*. 2009;193(6):W490-W6.
24. Grazioli L, Morana G, Federle MP, Brancatelli G, Testoni M, Kirchin MA, et al. Focal nodular hyperplasia: morphologic and functional information from MR imaging with gadobenate dimeglumine. *Radiology*. 2001;221(3):731-9.
25. Zech CJ, Grazioli L, Breuer J, Reiser MF, Schoenberg SO. Diagnostic performance and description of morphological features of focal nodular hyperplasia in Gd-EOB-DTPA-enhanced liver magnetic resonance imaging: results of a multicenter trial. *Investigative radiology*. 2008;43(7):504-11.
26. Kitao A, Zen Y, Matsui O, Gabata T, Kobayashi S, Koda W, et al. Hepatocellular carcinoma: signal intensity at gadoteric acid-enhanced MR imaging—correlation with molecular transporters and histopathologic features. *Radiology*. 2010;256(3):817-26.
27. Tsuboyama T, Onishi H, Kim T, Akita H, Hori M, Tatsumi M, et al. Hepatocellular carcinoma: hepatocyte-selective enhancement at gadoteric acid-enhanced MR imaging—correlation with expression of sinusoidal and canalicular transporters and bile accumulation. *Radiology*. 2010;255(3):824-33.
28. Gandhi SN, Brown MA, Wong JG, Aguirre DA, Sirlin CB. MR contrast agents for liver imaging: what, when, how. *Radiographics*. 2006;26(6):1621-36.
29. Seale MK, Catalano OA, Saini S, Hahn PF, Sahani DV. Hepatobiliary-specific MR contrast agents: role in imaging the liver and biliary tree. *Radiographics*. 2009;29(6):1725-48.
30. Chen B-B, Shih TT-F. DCE-MRI in hepatocellular carcinoma-clinical and therapeutic image biomarker. *World journal of gastroenterology: WJG*. 2014;20(12):3125.
31. Kloeckner R, dos Santos DP, Kreitner K-F, Leicher-Düber A, Weinmann A, Mittler J, et al. Quantitative assessment of washout in hepatocellular carcinoma using MRI. *BMC cancer*. 2016;16(1):758.
32. Feuerlein S, Pauls S, Juchems MS, Stuber T, Hoffmann MH, Brambs H-J, et al. Pitfalls in abdominal diffusion-weighted imaging: how predictive is restricted water diffusion for malignancy. *American Journal of Roentgenology*. 2009;193(4):1070-6.
33. Kele PG, van der Jagt EJ. Diffusion weighted imaging in the liver. *World journal of gastroenterology: WJG*. 2010;16(13):1567.
34. Sandrasegaran K, Akisik FM, Lin C, Tahir B, Rajan J, Aisen AM. The value of diffusion-weighted imaging in characterizing focal liver masses. *Academic radiology*. 2009;16(10):1208-14.